Electronic Supplementary Material (ESI) for ChemComm.

Supporting information

In-situ Reconstruction of Self-supported NiFeP Electrodes for Overall Water Splitting at Large Current Density

Ang Li, [a†] Dongcai Song, [a†] Runjie Cao, [b] Fangzheng Wang, [a] Hua Yan, [a] Hongmei Chen, *[a]

[a] College of Chemistry and Chemical Engineering, State Key Laboratory of Advanced Chemical Power Sources (SKL-ACPS), Chongqing University, Shazhengjie 174, Chongqing 400044, China.

[b] College of Polymer Science and Engineering, Sichuan University, No.29 Jiuyanqiao Wangjiang Road, Chengdu 610064, China

* Corresponding authors. Email: chenhongmei926@163.com. (H. M. Chen)

Experimental section

Materials

Nickel mesh was purchased from Qinghe Chengshuo Metal Materials Co., Ltd., (China). Commercial Pt/C/NM (20% wt%), RuO_2 and Nafion (5 wt%) were purchased from Sigma-Aldrich Chemical Reagent Co., Ltd. Sodium hydroxide (NaOH), nickel chloride hexahydrate ($NiCl_2·6H_2O$), ferrous chloride tetrahydrate ($FeCl_2·4H_2O$), trisodium citrate ($Na_3C_6H_5O_7·2H_2O$), boric acid (H_3BO_3), sodium hypophosphite ($NaH_2PO_2·H_2O$), and ammonium chloride (NH_4Cl) were provided by Shanghai Titan Science & Technology Co., Ltd. All reagents were used as received. The water used throughout all experiments was deionized.

Synthesis of 1st-NiFe/NM electrode

The nickel mesh (2.0 × 2.0 cm^2) was first cleaned ultrasonically in ethanol for 30 min, and then treated with 1.0 M $H_2C_2O_4$ aqueous solution at 80 ℃ for 1 h to remove the impurities and oxides layer. Finally, the nickel mesh was rinsed with deionized water before being stored in ethanol solution for use. To achieve the 1st-NiFe/NM electrode, mono-pulse electrodeposition was carried out in a two-electrode electrochemical system equipped with cleaned NM as the working electrode and nickel sheet as the counter electrode. The electrolyte was prepared with 0.1 M $NiCl_2·6H_2O$, 0.1 M $FeCl_2·6H_2O$ and NH_4Cl of different concentrations. According to the preliminary experiments, the operation temperature was kept at 30 ℃, the current density at 250 mA cm^{-2} and the turn-on (T_{on}) and turn-off (T_{off}) times were set at 20 and 10 ms, respectively. The effect of NH_4Cl concentration (0.5 M, 1.0 M, 2.0 M, 3.0 M) and deposition time (0 s, 300 s, 600 s, 1200 s, 1800 s, 2400 s) on morphology of the electrodes was investigated. The as-prepared 1st-NiFe/NM electrode was then washed with water and dried in air at room temperature.

Synthesis of 2rd-NiFe/NM electrode

The 2rd-NiFe/NM electrode was acquired by mono-pulse electrodeposition in a two-electrode electrochemical system with the 1st-NiFe/NM as the working electrode and nickel sheet as the counter electrode. The electrolyte solution consisted of 0.2 M $NiCl_2·6H_2O$, 0.2 M $FeCl_2·6H_2O$, 0.25 M $Na_3C_6H_5O_7·2H_2O$ and 0.3 M H_3BO_3. The deposition temperature was 30 ℃, the deposition current density was 50 mA cm^{-2}, and the T_{on} and T_{off} were both 10 ms with a total time 600 s. With other experimental conditions fixed, the effects of pulse frequency f (50 Hz,

5 Hz, 0.5 Hz, 0.05 Hz) and on-off ratio T_{on} /T_{off} (4:1, 3:1, 2:1, 1:1, 1:2, 1:3, 1:4) were investigated.

Synthesis of NiFeP/NM electrode

The 2rd-NiFe/NM and 0.8 g $NaH_2PO_2·H_2O$ were put in two clean porcelain boats. The one with $NaH_2PO_2·H_2O$ was placed at the upstream of the tube furnace (near the inlet end), and the other with the 2rd-NiFe/NM at the downstream (near the outlet end). The furnace was heated to 550 ℃ at a heating rate of 5 ℃ min^{-1} and maintained for 4 h in N_2 atmosphere (50 sccm). Then the reaction system was cooled naturally down to room temperature in the furnace to obtain the final NiFeP/NM with a load mass of 8 mg cm^{-2}.

Synthesis of Pt/C/NM/NM and RuO_2/NM

4 mg of 20 wt% Pt/C/NM and RuO_2 powder was dispersed in a mixture containing 470 μL of ethanol and 30 μL of Nafion solution to form slurry. 20 w % Pt/C/NM and RuO_2 was prepared by dipping the slurry onto a piece of Ni mesh with a real loading of 2 mg cm^{-2}.

Characterization

Powder X-ray diffraction (PXRD) data were obtained using a PAN-alytical X' pert diffractometer with Cu K α radiation (λ = 1.5418 Å). The morphology and chemistry of the samples were characterized by a field emission scanning electron microscopy (FE-SEM) (model JSM-7600 F, JEOL Ltd., Tokyo, Japan). Transmission electron microscopy (TEM) measurements were performed on a HITACHI H-8100 electron microscopy (Hitachi, Tokyo, Japan) with an accelerating voltage of 200 kV. The energy dispersive X-ray (EDX) mapping was carried out to detect the element composition and distribution. X-ray photoelectron spectroscopy (XPS) measurements were conducted by using a Thermo ESCALAB 250Xi with an Al K α (1486.6 eV) X-ray source on the samples with binding energies referenced to adventitious carbon at 284.8 eV. Raman spectra were acquired on a HORIBA LabRAM HR Evolution spectrometer under an excitation of 532 nm laser.

Electrochemical measurements

The three-electrode test system and Autolab (AUT72703) electrochemical workstation were employed to test the electrodes of interest. The as-prepared catalysts, commercial Pt/C/NM (20 wt %) and RuO_2 on nickel mesh (1.0 × 1.0 cm^2) were individually used as the working electrodes, the Hg/HgO (1.0 M KOH) electrode as the reference electrode, and a graphite plate as the counter electrode. Before HER test, the cyclic voltammetry (CV) test was first performed in a potential range of 0.1 V to − 0.4 V (vs. RHE), with a sweeping speed of 50 mV/s and a

duration of at least 30 cycles to stabilize the electrode. Then the scanning speed was changed to 1 mV/s and the potential range to 0.1 V to -0.9 V (vs. RHE) in 6 M KOH to obtain the linear voltammetry (LSV) curve. Before OER test, the scanning parameters of cyclic voltammetry (CV) were set as follows: the potential interval was 1.2 – 1.8 V (vs. RHE), and the scanning speed was 50 mV/s for at least 30 cycles to stabilize the electrode. Then the scanning speed was reset at 1 mV/s within 2 – 1.0 V (vs. RHE) to perform the linear Voltammetry scan (LSV). To evaluate the electric double layer capacitance for HER, cyclic voltammetry (CV) was conducted at a scanning speed of 5 – 32 mV/s within 0.02 – 0.12 V (vs. RHE); in the case of OER, the scanning was carried out at 5 – 29 mV/s in 1.11 – 1.21 V (vs. RHE). The performance of overall water splitting was assessed in a two-electrode system, where the optimized NiFeP/NM was utilized as the anode and cathode. Regarding electrochemical impedance test, the AC impedance method was employed. The high and low frequency range was 10^5 - 0.01 Hz, the bias applied in HER was – 0.2 V (vs. RHE) and the overpotential measured in OER was 1.55 V (vs. RHE). Chronopotentiometry was applied to evaluate the stability of electrode materials for HER. In the constant current tests of HER, OER and overall water splitting, the current density was set at 500 mA cm^{-2}.

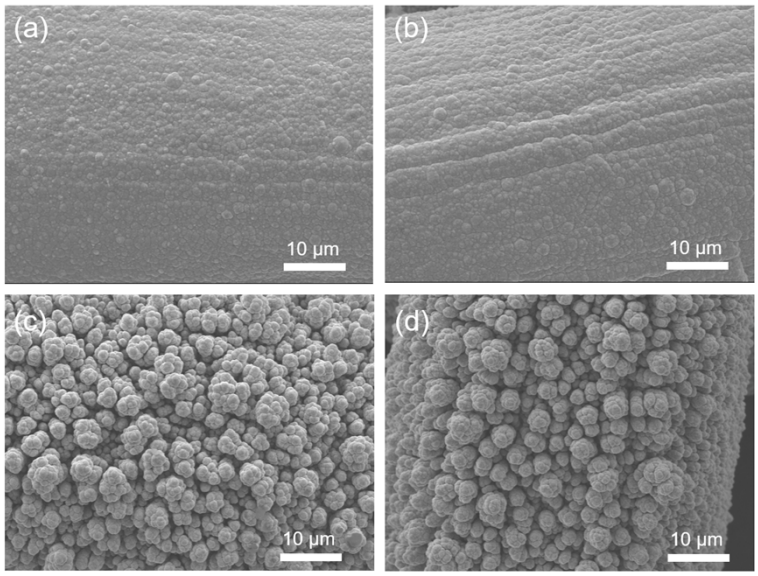

Figure S1. SEM images of 1st-NiFe/NM at different NH_4Cl concentrations: (a) 0.5 M, (b) 1.0 M, (c) 2.0 M, (d) 3.0 M.

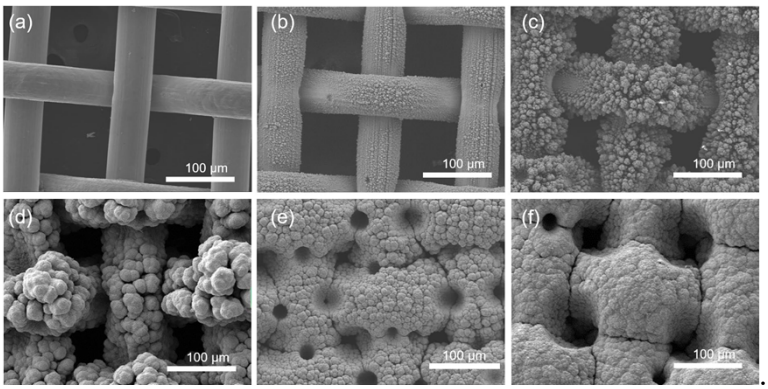

Figure S2. SEM images of 1st-NiFe/NM at different pulse electrodeposition time: (a) 0 s, (b) 300 s, (c) 600 s, (d) 1200 s, (e) 1800 s, (f) 2400 s.

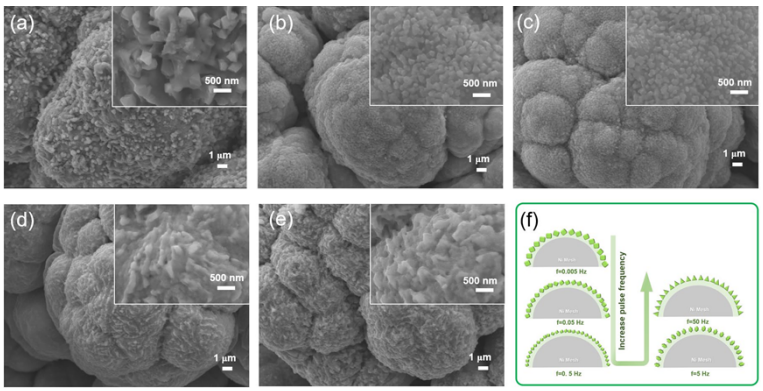

Figure S3. SEM images of NiFeP/NM at different frequencies: (a) 0.005 Hz, (b) 0.05 Hz, (c) 0. 5 Hz, (d) 5 Hz, (e) 50 Hz; (f) Schematic diagram of morphologies at different frequencies.

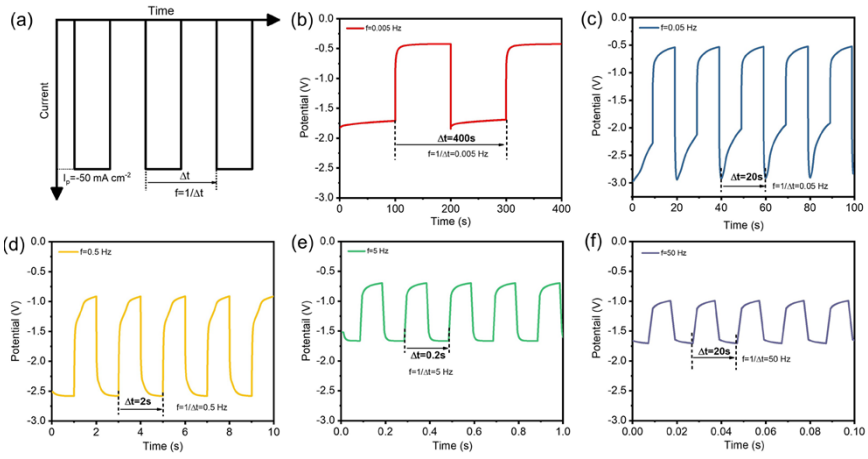

Figure S4. (a) Current-time curve of applied pulsed current; Potential-time curve of response at different frequencies: (b) 0.005Hz, (c) 0.05Hz, (d) 0. 5Hz, (e) 5Hz, (f) 50Hz.

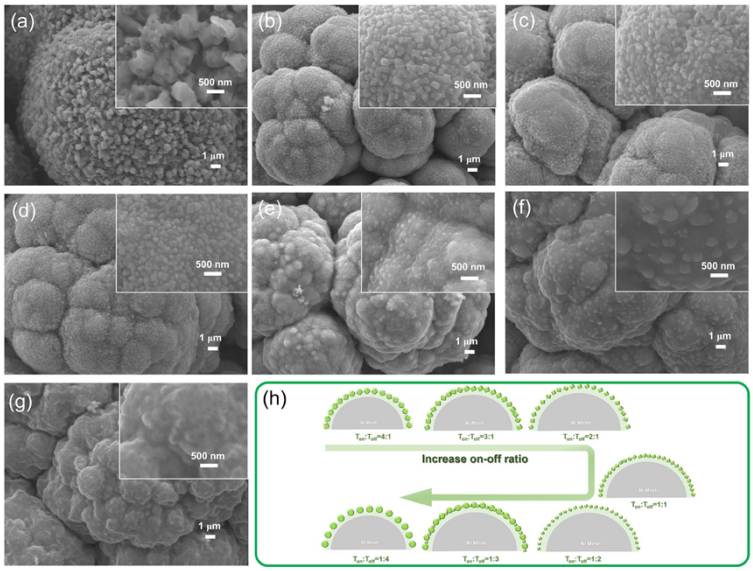

Figure S5. SEM images of NiFeP/NM electrode at different on-off ratios: (a) T_{on} : T_{off} = 4:1, (b) T_{on} : T_{of} = 3:1, (c) T_{on} : T_{of} = 2:1, (d) T_{on} : T_{of} =1:1, (e) T_{on} : T_{of} = 1:2, (f) T_{on} : T_{of} = 1:3, (g) T_{on} : T_{of} = 1:4; (h) Schematic diagram of morphologies at different duty ratios.

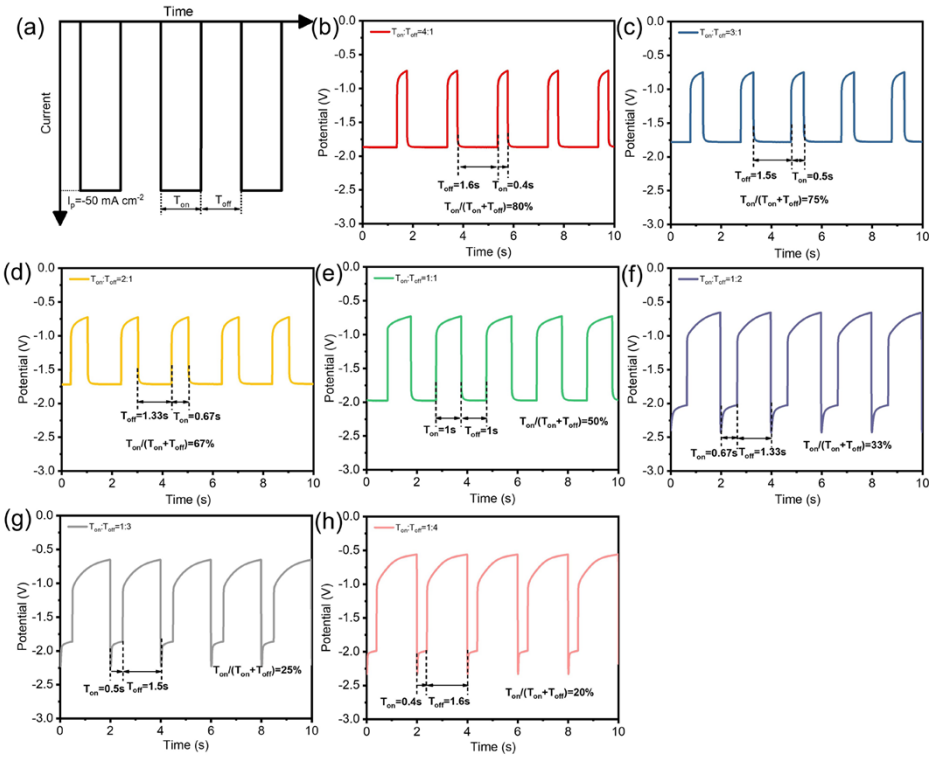

Figure S6. (a) Current-time curve of applied pulsed current; Potential-time curve of response at different duty ratios: (b) T_{on} : T_{of} = 4:1, (c) T_{on} : T_{of} = 3:1, (d) T_{on} : T_{of} = 2:1, (e) T_{on} : T_{of} = 1:1, (f) T_{on} : T_{of} =1:2, (g) T_{on} : T_{of} = 1:3, (h) T_{on} : T_{of} = 1:4.

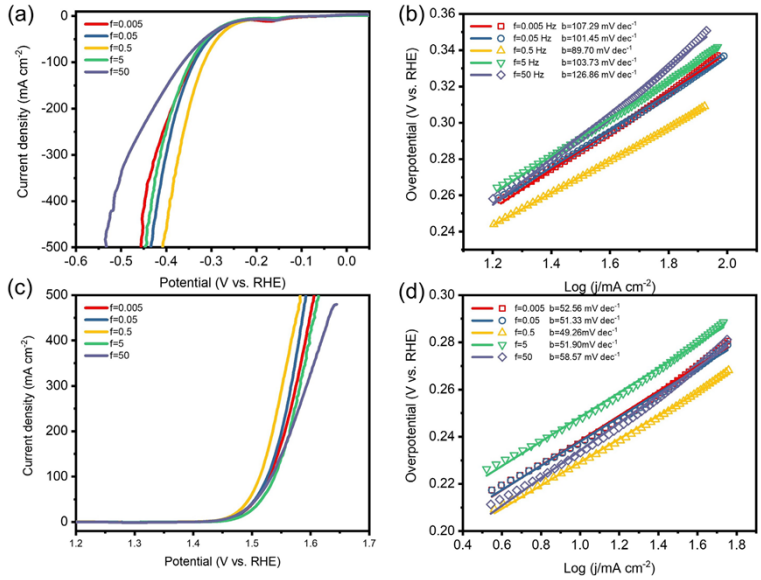

Figure S7. (a) Cathodic polarization curves at different frequencies in 6.0 M NaOH solution; (b) Corresponding HER Tafel slope curves; (c) Anode polarization curves for different frequencies in 6.0 M NaOH solution; (d) Corresponding OER Tafel slope curves.

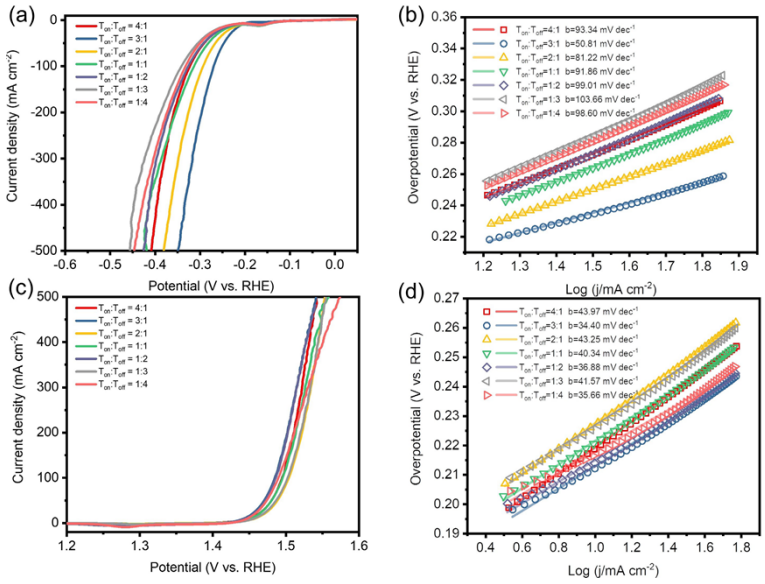

Figure S8. (a) Cathodic polarization curves at different duty ratios in 6.0 M NaOH solution; (b) Corresponding HER Tafel slope curves; (c) Anode polarization curves for different duty ratios in 6.0 M NaOH solution; (d) Corresponding OER Tafel slope curves.

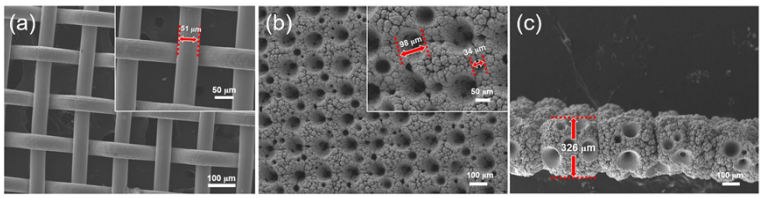

Figure S9. SEM images of catalysts at low magnification: (a) NM, (b) the surface of NiFeP/NM electrode, (c) the transverse surface of NiFeP/NM electrode.

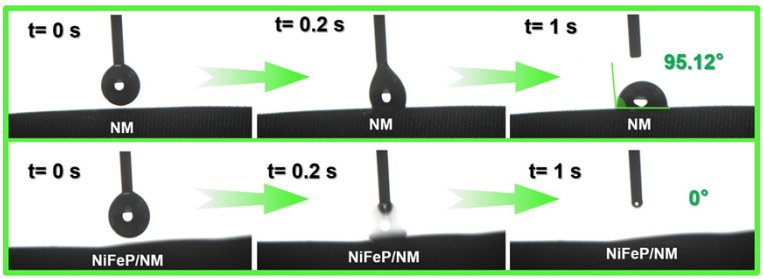

Figure S10. The contact angles of water droplets on NM and NiFeP/NM electrodes.

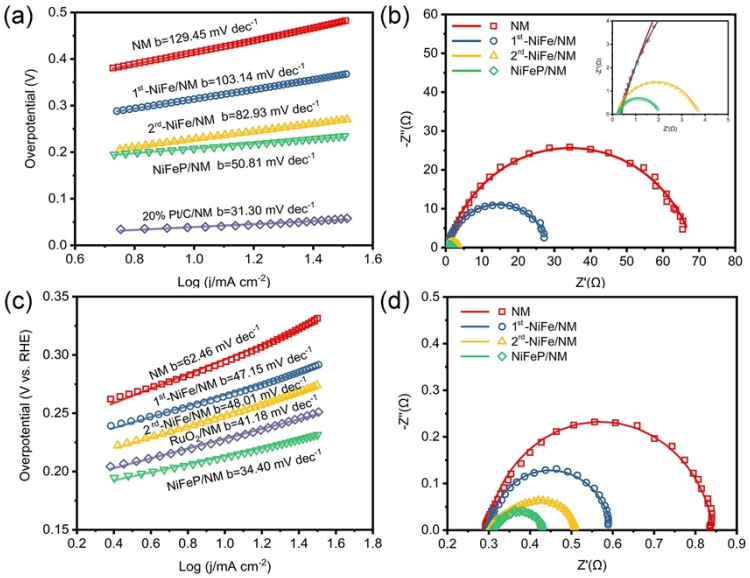

Figure S11. Corresponding Tafel slopes and Nyquist plots for HER (a, b) and OER (c, d).

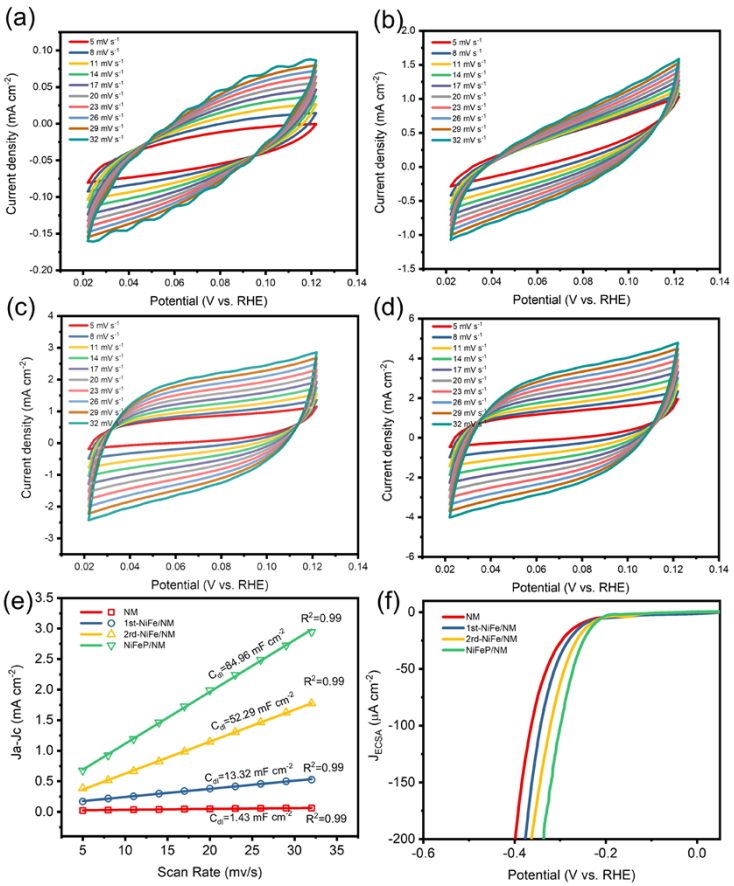

Figure S12. Cyclic voltammograms (CVs) for (a) NM, (b) 1st-NiFe/NM, (c) 2rd-NiFe/NM, (d) NiFeP/NM in the range of HER non-faraday capacitive currents with sweeping rates from 5 to 32 mV s^{-1}; (e) Double layer capacitance curves for NM, 1st-NiFe/NM, 2rd-NiFe/NM and NiFeP/NM; (f) Normalized LSV curves by ECSA.

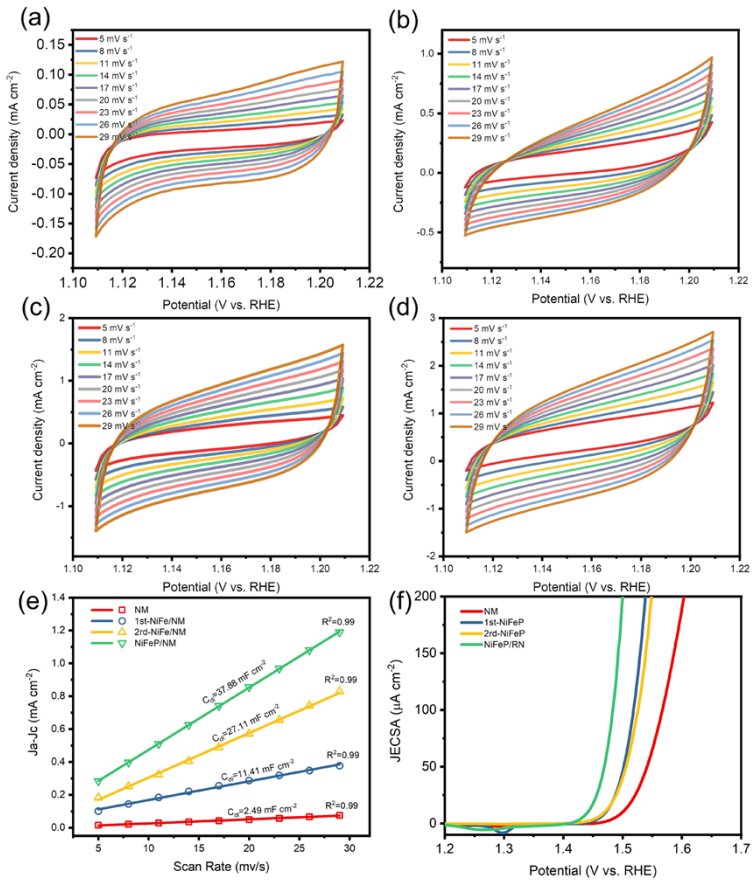

Figure S13. (a-d) NiFeP/NM in the range of OER non-faraday capacitive currents with sweeping rates from 5 to 29 mV s^{-1}; (e) Double layer capacitance curves for NM, 1st-NiFe/NM, 2rd-NiFe/NM and NiFeP/NM; (f) Normalized LSV curves by ECSA.

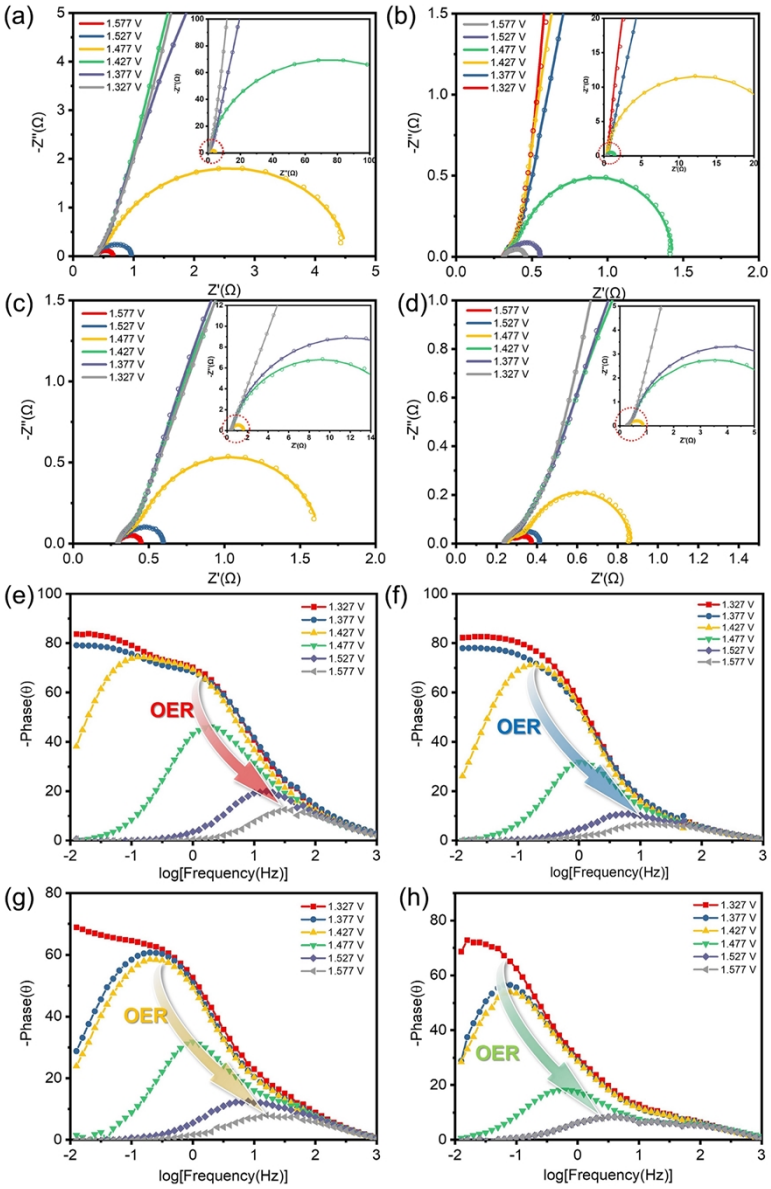

Figure S14. (a-d) Nyquist plots and (e-h) Bode plots for NM, 1st-NiFe/NM, 2rd-NiFe/NM and NiFeP/NM electrodes at various voltages for OER.

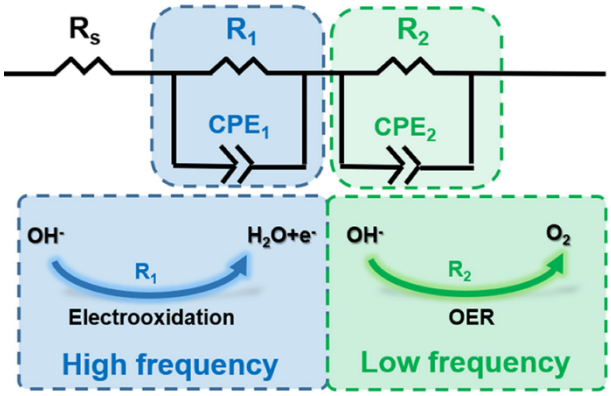

Figure S15. Electrical equivalent circuit model used for analyzing the interfacial charge transfer, Nyquist plots at different voltages.

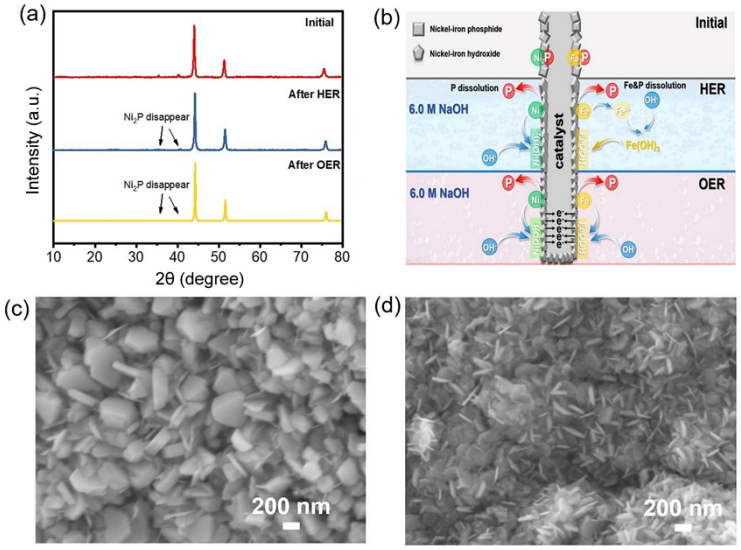

Figure S16. (a) XRD of NiFeP/NM; (b) Schematic diagram of surface reconfiguration that may occur during HER and OER tests in 6.0 M NaOH solution; (c) SEM of NiFeP/NM electrode after HER test; (d) SEM of NiFeP/NM electrode after OER test.

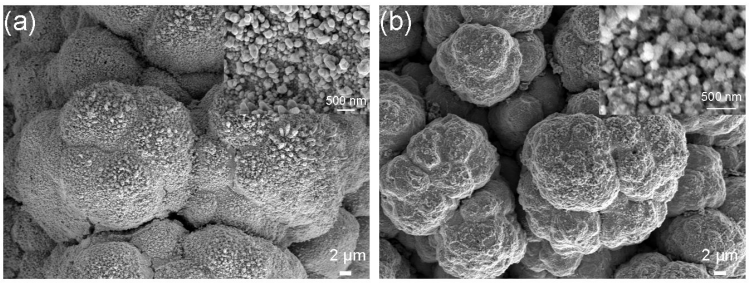

Figure S17. SEM images of NiFeP/NM after 100 h @ 500 mA cm $^{-2}$ stability test for (a) HER and (b) OER.

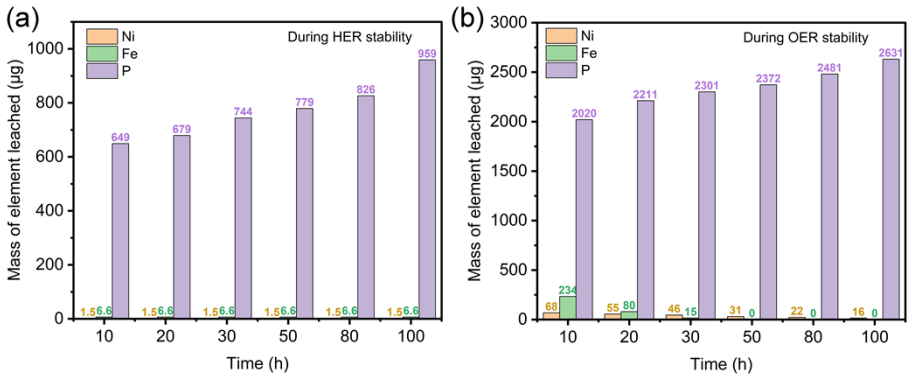

Figure S18. The mass of leached Ni and Fe in electrolyte during a constant current stability test of 500 mA cm^{-2} for 100 h.

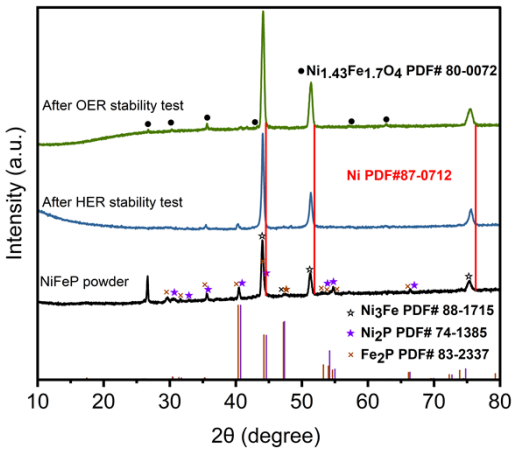

Figure S19. Powder XRD pattern of NiFeP/NM before and after OER stability test.

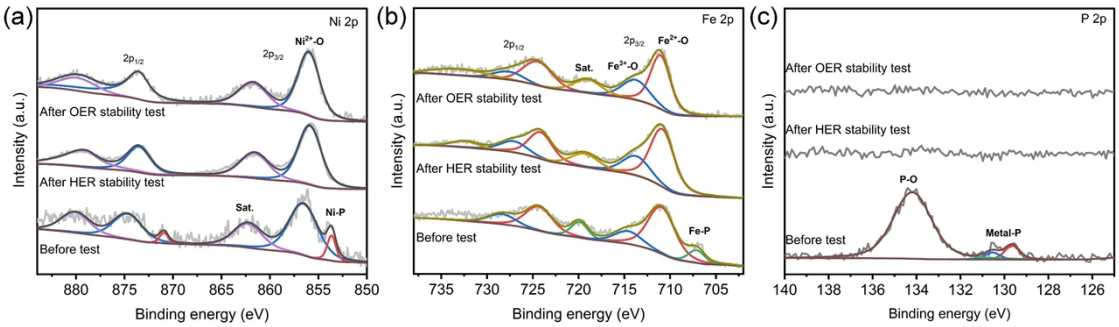

Figure S20. XPS of NiFeP/NM before and after 100 h stability test under 500 mA cm^{-2}: (a) Ni 2p, (b) Fe 2p and (c) P 2p.

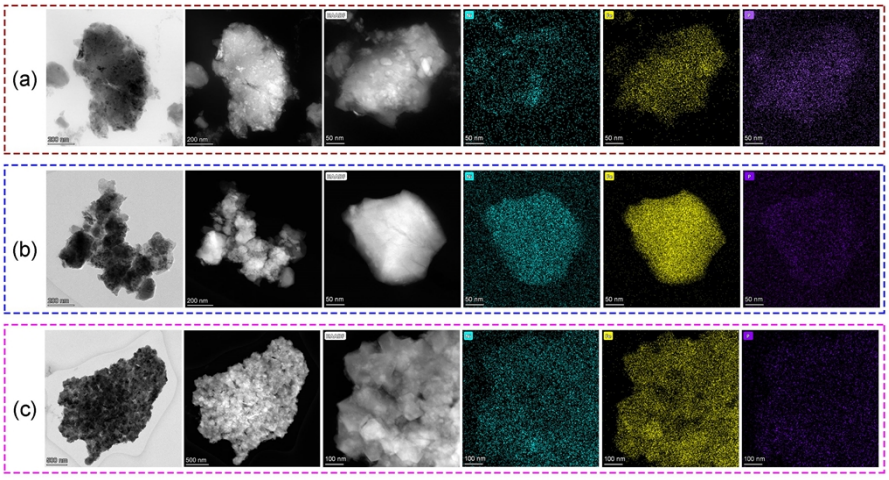

Figure S21. TEM image, STEM image, HADDF image and EDS mapping of NiFeP/NM before and after 100 h stability test under 500 mA cm^{-2}: (a) before test, (b) after HER stability test and (c) after OER stability test.

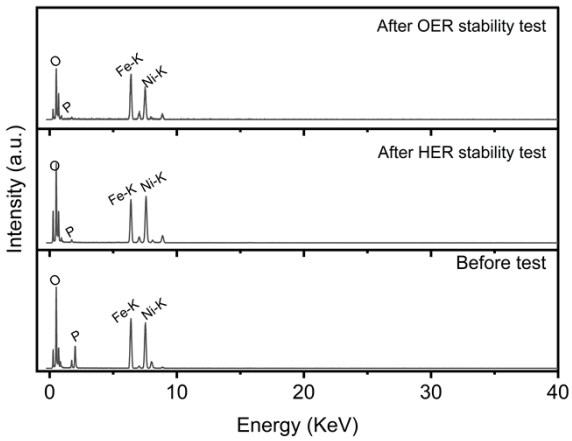

Figure S22. TEM-EDS of NiFeP/NM before and after 100 h stability test under 500 mA cm^{-2}.

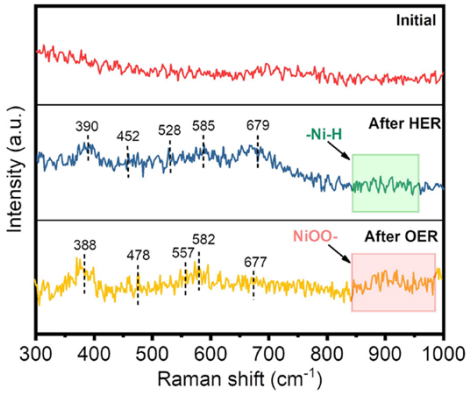

Figure S23. Raman spectra of NiFeP/NM electrode before and after HER and OER stability test.

Table S1. Electrochemical specific surface area parameters of different catalytic electrodes.

Electrodes	NM	1st-NiFe/NM	2rd-NiFe/NM	NiFeP/NM
C_{dl} (mF cm^{-2})	1.43	13.32	52.29	84.96
ECSA (cm^{2})	35.75	333.00	1307.25	2124.00